HEAT TRANSFER MECHANISM IN A-SI AND A-SIH

A thesis
Presented to
the faculty of the school of Engineering and applied science
University of Virginia

In partial fulfillment
of the requirements for the degree

Master of Science

By Mehrdad Fazli
Advisor: Keivan Esfarjani

August 2019

Acknowledgment

I am extremely thankful to my advisor Prof. Keivan Esfarjani for all the help and patience and guidance he showed along this long way. This work would not be possible without his help and support. It means a lot to me. I also thank my committee members that I learned very much from them.

I also want to appreciate my family who supported and motivated me all the time from thousands of miles away. I owe everything to them and their support.

I would like to especially thank a friend who helped me a lot but is not with us now. I want to dedicate this to the memory of my amazing friend Rouzbeh Rastgarkafshgarkolaei whose memory is always alive in our hearts.

I owe a lot to my lovely girlfriend, Tirajeh. I cannot put in words the amount of support and patience she offered to me.

Table of Contents

Abstract

Disordered solids are important materials to study because of their broad applications in technologies like thin-film transistors (TFT), solar cells and etc. They also have a scientifically significance due to their complexity and lack of order and periodicity. One of the long-standing issues in this class of solids is understanding the nature of heat transport in these solids. The common model of phonon gas breaks down for these materials. Therefore, many theories have formed around explaining the physics of these materials.

In this study, we used molecular dynamics simulations to investigate the thermal transport in amorphous silicon. We also looked into the hydrogenated amorphous silicon and microscopically investigated the effect of hydrogen doping in a-Si. We have also studied the evolution of the structures as the hydrogen content changes in a-SiH.

Our results suggest that hydrogenated amorphous silicon can demonstrate fundamentally different capabilities compared to a-Si. Thermal conductivity, calculated using Green-Kubo formula, shows that hydrogens can increase the thermal conductivity. We also separated the effect of hydrogen atoms and silicon atoms to fathom the role of hydrogen atoms. Most of our results are compared well with prior works in this area and can be extended by measuring the modal contributions to thermal conductivity.

I. Introduction

Motivation and objectives

Amorphous materials also known as glass-like materials are of great importance in many technological applications. They are widely used in electronic devices like thin film transistors (TFT), optoelectronic devices like solar cells. Their main advantage over the crystalline materials is their flexibility, different thermal and mechanical properties, and relatively low cost of fabrication. These features have made them attractive materials for both scientific and industrial purposes. They have been studied since the mid-twentieth century. A lot of theoretical and experimental studies have emerged aiming at a better understanding of the physics of disordered materials. The lack of periodicity and order either translational or compositional makes this class of materials hard to explain theoretically. The quest to come up with a universal model to explain the physics behind these materials and thoroughly describe their behavior is still ongoing. The

Introduction

reason is that this seemingly solely scientific problem can give immense insight into the nature of heat transport in solids and help us better engineer these materials for specific purposes.

Amorphous silicon is one of the first amorphous solids that was used for engineering purposes and it has remained the most widely used material in many applications. In this report, our objective is to study amorphous silicon and also hydrogenated amorphous silicon with the aid of computer simulations to understand the heat transport mechanism in these solids. We also aim at evaluating the effect of hydrogen doping on the thermal properties of a-Si. The method that is used in this study is molecular dynamics simulations.

Amorphous solids can be divided into chalcogenide glasses and tetrahedrally bonded amorphous solids. Chalcogenide glasses are the ones containing chalcogen elements (sulfur, selenium, tellurium) [1]. Amorphous silicon and germanium are examples of tetrahedrally bonded amorphous materials. These materials drew a lot of attention both in scientific researches and industry the beginning in the 20th century.

Nowadays, amorphous semiconductors are ubiquitous due to the numerous applications in hardware electronics and optoelectronic technologies. A comprehensive account of the applications of amorphous materials has been reported in the literature [1][2]. Amorphous silicon and amorphous silicon-based compounds are the most famous and widely used of its family. Fig. 1 shows a typical amorphous hydrogenated silicon solar cell. The major difference between c-Si and a-Si that makes a-Si distinct is its flexibility, low thermal conductivity, and the low cost of its production. Due to this flexibility, we can make a-Si as thin as a few nanometers.

Introduction

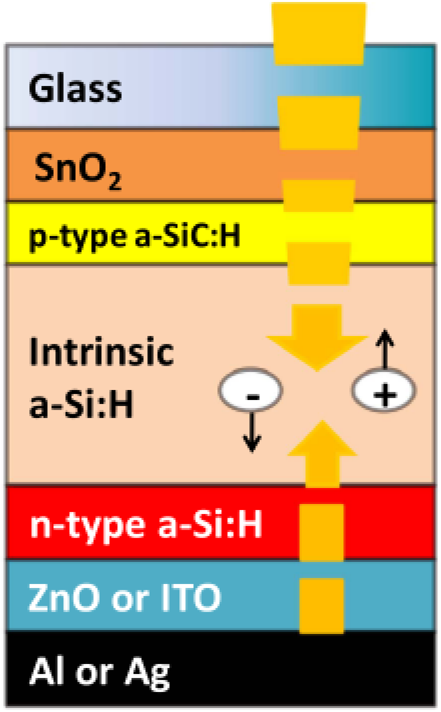

Fig. 1 Schematic of a a-SiH solar cell

In what follows we provide a short introduction to the heat transfer mechanisms in solids in general. Then we highlight the differences between the crystals and glasses and discuss the difficulties that arise when dealing with glass-like solids. Later we go over the past studies and models that were proposed to explain heat transfer in glasses.

Heat transfer mechanisms in solids

In many engineering designs and applications, heat transfer related problems remained as a bottleneck to further advancements. From dissipating excessive heat in microprocessors or internal combustion engines to avoiding heat loss in refrigerators and cooling systems are only a few examples of heat transfer problems. Usually, in heat transfer problems we are looking to minimize or maximize the heat flow in a material. This requires an in-depth knowledge of the heat transfer mechanism in materials. To this end, we first review the fundamental concepts in heat transfer.

Classically, heat transfer mechanisms are divided into three mechanisms namely conduction, convection, and radiation. Conduction is the heat transfer via the vibrations of atoms or the traveling of electrons. Convection is the heat transfer via the migration of particles inside a material. In radiation, energy is carried via the electromagnetic waves.

Unlike the fluids, in solids at equilibrium, due to the strong bonding of atoms/molecules, atoms/molecules are not allowed to move freely, rather they vibrate around their equilibrium positions. Therefore, there is no traveling of particles and thus no convection in solids. Also, unless having a very high temperature, radiation can be neglected compared to conduction which means the dominant heat transfer mechanism in solids is conduction.

If we apply a temperature gradient on two ends in a solid, the heat transfers from the hot region to the cold region. The mathematical formalism for this process is the Fourier law. Fourier law states that in the steady state, the rate of heat transfer is directly proportional to the temperature gradient. Meaning that if one applies a greater temperature gradient in a solid they get a higher heat transfer rate. The parameter that relates the heat transfer rate to temperature gradient is called the thermal conductivity and is denoted by κ.

$$\dot{q} = -\kappa \nabla T \tag{1-1}$$

Thermal conductivity

The thermal conductivity is the ability of a certain material to transfer the heat through itself. We can also define the inverse of the conductivity, as resistivity, which is the resistance of a given material to the heat flow. A deeper understanding of thermal conductivity requires honing in the microscopic description of the thermal conductivity in solids.

As was mentioned earlier heat transfers through a solid via vibrations of atoms or through the traveling of electrons. This means that in solids (crystals) we have two types of heat carriers; electrons and phonons (will be defined later). Subsequently, we can imagine that in thermal conductivity we have the contribution of both phonons and electrons. We then define phononic thermal conductivity, κ_p and electronic thermal conductivity, κ_e. In this study, we are focusing on on dielecteric and semiconductor materials. Hence, we don't use any subscript to differentiate between phononic and electronic thermal conductivity, instead we simply use κ to denote phononic thermal conductivity.

In conducting materials we have free electrons that can move freely and carry energy. Unlike in conductors, there is not free electrons in dielectric materials or semiconductors, therefore, the only heat carriers are vibrations of atoms. This makes the study of these vibrational modes very important for the semiconductors.

Traditionally the interaction of atoms within a material is simplified into a mass-spring picture (Fig. 2). Atoms are considered as point masses that are connected together via springs. Sprigs here, represent the stiffness of the atoms bondings.

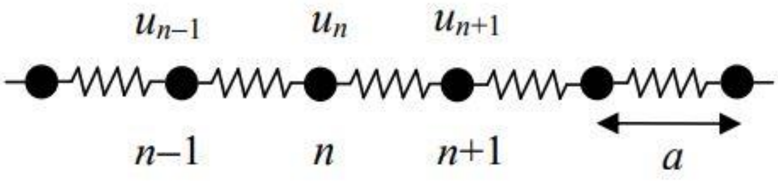

Fig. 2 Mass-Spring picture of 1D atom chain

This way the displacement of a single atom can excite the neighboring atoms and cause them to move. Therefore, vibrational modes can propagate throughout the structure like a wave. This microscopic picture provides a qualitative description of atomic vibrations and heat carriers. In a mass-spring system, the spring constant governs the motion of the mass subject to an exerted force. In a system of microscopic particles, the interatomic potential is conceptually equivalent to the spring constant and it determines how the particles interact in the system. Forces on one particle can be easily calculated by differentiating the potential energy with respect to displacements of atoms. Within harmonic approximation and at the equilibrium the potential can be approximated by a quadratic function of the displacements, meaning that the higher order displacement dependent terms will be omitted. It is worth noting that considering small displacements for atoms around equilibrium positions, the harmonic approximation is a valid assumption and generates satisfactory results. In Fig. 3 the potential energy between two particles is schematically depicted.

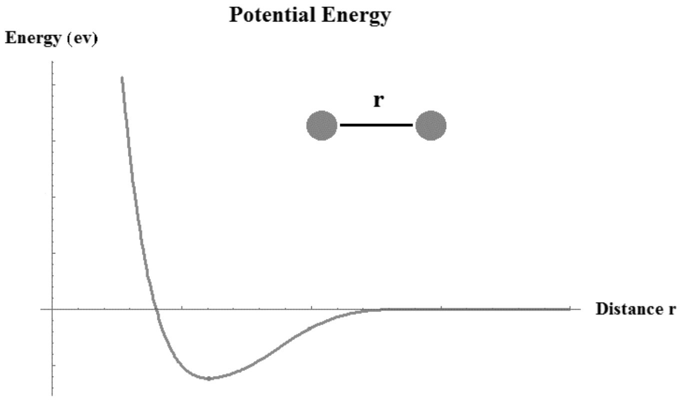

Fig. 3 Schematic of the potential energy vs distance for two particles. Potential Energy has attractive and repulsive parts. Repulsive is the left side of the equilibrium distance and attractive is its right side.

The total potential energy in the system is indeed its potential energy at the ground state (all particles at their equilibrium positions) plus the potential energy induced by the displacement of the particles. Like in the mass-spring case, a tiny displacement in the position of the mass results in stored potential energy in the spring. So one can write:

$$U = \frac{1}{2} \sum_{i,j,i \neq j} U_{ij} \tag{1-2}$$

$$F_i = -\nabla_{\mathrm{i}} U \tag{1-3}$$

$$m_i \frac{d^2 u_i}{dt^2} = F_i \tag{1-4}$$

In equation (1-2), U_{ij} is the potential energy between i and j particles, and $u_i = X_i^t - X_i^0$ is the infinitesimal displacement of atom i with respect to its equilibrium position. This system of equations can be solved analytically for the entire system. For example for a 1D chain of atoms vibrating at frequency ω the solutions are of the form:

$$u_i = \sum_{\omega} A_\omega e^{i(-\omega t + k x_i)} \tag{1-5}$$

Here A is the amplitude of vibrations and ω is the frequency of the vibrations and k is the wavevector and x_i is the equilibrium position of the ith atom which is a multiple of a, lattice constant. Wavevector determines the direction of the propagation of the waves and its magnitude denotes a point in the lattice. We can have a broad range of vibrational modes in different directions all characterized by their wavevectors and frequencies. Lattice vibrations carry energy and this energy is quantized. Each quantum of energy is called "phonon". This terminology is used in the analogy of photons that are quantum energy of electromagnetic waves. Likewise, phonons can be treated as moving particles or heats carriers.

Now that the definition of phonon is clear we can provide a formula for the thermal conductivity. The kinetic theory yields a microscopic and quantitative description of the thermal conductivity for dielectric materials:

$$\kappa = \frac{1}{3} C v \Lambda \tag{1-6}$$

Where Λ is the mean free path (MFP) of phonons, defined as the distance that a phonon can travel before it is scattered. v is also the sound velocity in the material and C is the heat capacity. Equation (1-6) can easily be driven from the heat conduction equation.

Also one can define the phonon's lifetime (or scattering time) similar to phonon's MFP which is the time between two scattering events. Then we can rewrite the equation (1-6) as:

$$\kappa = \frac{1}{3} C v^2 \tau \tag{1-7}$$

It is worth mentioning that phonon scattering is a very crucial phenomenon that governs the thermal conductivity in solids. Phonons can get scattered by Umklapp process, impurities, defects, electrons, boundaries and themselves. More scattering sources and higher scattering rate would diminish the thermal conductivity by reducing the mean free path. We will not go into the details of the scattering processes but to get some insight it is good to provide the Matthiessen's rule to clarify how scattering can affect the thermal conductivity. Matthiessen's rule combines several scattering types as:

$$\frac{1}{\tau} = \frac{1}{\tau_1} + \frac{1}{\tau_2} + \frac{1}{\tau_3} + \cdots \tag{1-8}$$

Here τ_i is the scattering time of the ith type. It now becomes clear that more terms on the right hand side of the equation reduces the total scattering time and thus the thermal conductivity (eq. (1-7)). That is part of the reason that disordered materials have generally lower thermal conductivity.

The idea of treating phonons like a gas of moving particles (heat carriers) is called phonon gas model (PGM). Theories based on phonon gas model decently capture the thermal properties of crystals and ordered materials and exhibits excellent performance in explaining the nature of heat transfer in these materials. But, in disordered materials, we do not have a lattice and we cannot think of wavelike displacements of atoms. The heat carriers are still vibration of atoms although they are not traveling wave-like with well-defined wavevectors. In fact, due to the lack of the translational symmetry, the concepts of group velocity, wavevector and mean free path (MFP) are not well-defined. In disordered materials a majority of vibrations do not propagate throughout the material, rather many of the vibrational modes are temporarily stationary and localized. Hence we cannot use the terminology of phonon for the disordered materials, instead, three different vibrational regimes will be defined. We now overview the theories on the thermal transport in disordered materials beginning from Einstein theory.

Prior works

Probably the first attempt to explain the thermal transport in solids is Einstein work. He proposed that in solids at equilibrium atomic vibrations are harmonic oscillators. Also, he states that the coupling of these oscillators is the means of heat transport. Therefore, for an imaginary material that the atomic vibrations are not coupled the thermal conductivity is zero [3]. In the Einstein theory, the heat carriers are coupled vibrations of neighboring atoms that can be considered to randomly walk within the material. Building upon the Einstein model, Slack proposes a model for the lower limit of the thermal conductivity in disordered solids [4]. This model proved to be consistent with numerous experimental studies although later, some studies cast doubt on the validity of such a model by investigating the thermal conductivity of a-Si or other silicon-based compounds [5][6][7].

Years after Einstein, Allen and Feldman (A-F) [8] proposed another theory that achieved great success in explaining the heat transport in amorphous materials. They categorized the vibrational modes to extended and localized modes. Extended modes then were further divided into diffusons and propagons. Localized modes are called locons. Propagons are plane-wave-like modes and resemble phonons in crystals. They can propagate throughout the material with sound velocity. They are expected to contribute greatly to the thermal conductivity even though the fraction of propagating modes are much lower than diffusons and locons. Locons, on the other hand, are localized modes that cannot travel far and get scattered quickly. Therefore, they have a negligible contribution to thermal conductivity. Diffusons have a mid-range of the MFPs and are the major contributors to the thermal conductivity mostly because they constitute the majority of vibrational modes. There is not a clear cut between these modes and they are spread out on a spectrum which makes it hard to characterize them. In fact, characterizing these three different vibrational regimes and computing their contribution to thermal conductivity is a controversial matter and has been subject to many studies lately.

A-F theory also suggests a formula for thermal conductivity which is based on the modal specific heat and diffusivity as:

$$\kappa = \frac{1}{V}\sum_{i} C_i(T)D_i \tag{1-9}$$

In most studies in the literature, propagons are considered to form less than 5% of the modes and have frequencies of a few THz but contribute to 20% to 50% [9][10][11] of the thermal conductivity of a-Si. These studies suggest that the dominant heat carriers are diffusons while Moon and Minnich [12] claimed that the propagating modes are the major contributors to thermal conductivity. They used the dynamical structure factor to show that propagons extend up to the frequency of 10 THz and are the dominant heat carriers in a-Si. Lv and Henry [13] also calculated the contributions of the different modes and found out that the contribution of localized modes to thermal conductivity in a-SiO_2 is over 10%.

Allen Feldman theory shines a light on the nature of the vibrational modes in amorphous solids but gives rise to another challenge which is to distinguish between these three regimes and measure their role in the thermal conductivity. Localized modes can be distinguished via the participation ratio which is a measure of how a mode is localized [14]:

$$PR_n = \frac{\left(\sum_i \vec{e}_{i,n}^{\,2}\right)^2}{N\sum_i \vec{e}_{i,n}^{\,4}} \tag{1-10}$$

Where $\overrightarrow{e_{\iota,n}}$ is the eigenvector of mode n and atom i.

Differentiating between diffusons and propagons is not as straightforward though. Seyf and Henry [15] suggested using Eigenvector periodicity (EP) to distinguish between the diffusons and propagons. This is so far the most systematic way of differentiating between diffusons and propagons and they tested it on a-Si vs c-Si. One of the importance of the EP is that it ranges from 0 to 1. A value close to 1 indicates propagating modes and close to 0 indicates diffusons.

Another seminal work in the search for a structured way to calculate the modal contributions to thermal conductivity was done by again Lv and Henry [16]. They based off their model on the Green-Kubo formula for the thermal conductivity and used the lattice dynamics formalism to decompose the heat current.

$$Q(n,t) = \frac{1}{V}\sum_{i}\left[E_i\dot{x}_i(n,t) + \sum\nolimits_{j}\left(-\nabla_{r_i}\phi_j . \dot{x}_i(n,t)\right) r_{ij}\right] \tag{1-11}$$

Where E_i is the sum of the kinetic and potential energy of atom i, $x_i(n,t) = \frac{1}{\sqrt{m_i}} P_j(n)X(n,t)$ where $P_j(n)$ is the polarization of jth atom and n is the mode index.

Then they substitute the mode-dependent heat current in equation (1-11) in the Green-Kubo formula to find the total thermal conductivity as the summation of modal thermal conductivity over all modes. The fundamental distinction of this approach is that it does not require the assumption of PGM. Consequently, their method does not rely on the definition of the group velocity for heat carriers. They showed that their method reproduces the results of the AF method for a-Si.

Recently, Isaeva and Baroni [17], proposed a unified formalism called quasi-harmonic Green-Kubo (QHGK), to model the heat transport in crystals as well as disordered materials. Their model is based on the Green-Kubo theory of linear responses and interpolates between Boltzmann-Peierls theory for crystals and A-F theory for disordered systems.

There are also some interesting works on a-SiH and its thermal and structural properties. Liu et al. [18] fabricated a $80\mu m$ thick hydrogenated amorphous silicon via hot-wire chemical-vapor deposition. They found that the thermal conductivity of their a-SiH to be anomalously high ($4\ W/mK$) at around room temperature. Sriraman et al. [19] also studied the a-SiH both experimentally and numerically using molecular dynamics. They manufactured their samples using a plasma deposition technique. They found that the introduction of the hydrogen to the a-Si leads to the crystallization of a-Si.

II. Molecular Dynamics Simulations

Molecular dynamics (MD) simulation is a way to simulate the interactions of the particles in a given system. MD is a powerful tool developed over half a century ago to study materials on the molecular and atomic scale but only became so widespread in the last two decades thanks to the enormous increase in the computational power of computers. MD is a classical technique based on the solving of Newton's equations of motion for a system consisting of interacting particles. In molecular dynamics, particles are treated as point masses that can interact with each other through the interatomic potentials. As we mentioned earlier, having the interatomic potential between particles of material can provide us with a sufficiently accurate and complete description of the material properties. Once the interatomic potential is known the MD simulations are nearly experiments and they can even be used to predict the properties of structures.

Molecular dynamics like every other technique has its own strengths and weaknesses. Since MD is governed by classical physics and solves Newtonian equations of motion, it can handle large supercells or cluster of atoms rapidly. Today MD simulations of medium size supercells (ten or hundreds of nanometers) for a few nanoseconds can even be performed on personal computers. Although MD is a powerful tool, it cannot be applied to all classes of materials and is not as accurate as methods like Density Functional Theory (DFT) which is based on quantum mechanics. Yet MD yields reasonably good results for large molecules and disordered systems and even some crystals or alloys and in that, it is an extensively used tool in chemical physics, materials science, and biomolecules.

Inputs of MD simulations are the initial conditions, including initial positions and velocities, interatomic potential, and the constraints on the system. The challenging part of an MD simulation is to find an accurate interatomic potential which is able to capture the complexity of the interactions and produces acceptable results. MD simulation results are usually validated with the experimental results or methods with more accuracy like DFT. Many studies have been devoted to finding the best possible potential or to fit the parameters of existing potentials and optimize them for a specific material. These potentials can vary from simple two-body potentials, like Lennard-Jones, to many-body potentials, like Stillinger-Weber or Tersoff. More complex potentials are more computationally expensive but in return, they produce more reliable results.

Interatomic potentials have some parameters that let them adjust to a range of different materials. As the number of the parameters for an interatomic potential increases, it becomes more complex and evidently more flexible and more capable of capturing various properties of the material.

In an attempt to make MD simulations more accurate Ab-initio MD has evolved. In Ab-initio MD the force constants are calculated during the simulation using the first principle calculations. It greatly improves the accuracy of the MD simulations by calculating the parameters of the interatomic potential on the fly. The downside of Ab-initio MD is that it makes the simulations much more time and resource consuming.

Molecular Dynamics Simulations

Among all the MD packages Large-scale Atomic/Molecular Massively Parallel Simulator (LAMMPS) developed by the Sandia National Laboratories and General Utility Lattice Program (GULP) [20] are the most common ones. LAMMPS is a very efficient MD package due to its parallelization, therefore, all the MD simulations in the current study have been performed using LAMMPS. Also, for the visualizations, we used an open-source visualization tool, OVITO [21].

Creating structures in LAMMPS

To create the amorphous silicon samples we started off from the crystalline silicon. A conventional way to create amorphous structures is to melt and quench the crystalline structure. We also used this method for both a-Si and a-SiH samples. A-Si was created via melting a diamond structure silicon by raising the temperature well above its melting point to ensure that atoms are completely randomized. In this case, the temperature was raised to 3000K. We then dropped the temperature abruptly in three steps to 2000K, 1000K and finally 300K. The structures maintained for some tens of ps at each stage to let them reach their most stable state at that temperature. This is done by an isobaric and isothermal ensemble (NPT). At the end of the simulations, the structures were minimized and frozen to their ground state with zero kinetic energy (Fig. 6).

For the case of a-SiH, we again used the diamond c-Si as our base structure. Then hydrogen atoms were randomly placed in the supercell. The number of hydrogens was determined from the target hydrogen content. By fixing the number of the silicons we can claim that the masses of the a-SiH structures are relatively identical. To ensure that the hydrogens have enough time to find their places we kept the structure at a high temperature for a longer time so that hydrogens reach their optimal positions.

For a-Si, we used both Stillinger-Weber and Tersoff potentials for our MD simulations. A-SiH structures were all simulated using Tersoff potential. The Tersoff potential is a three-body empirical potential proposed by J. Tersoff [22] and consists of attractive and repulsive terms and accounts for bond order and bond angle. It is a flexible potential and has been used to model many multi-component systems including SiH. Ohira et al. [23] fitted the parameters of the Tersoff potential for SiH and most of the computer simulation works that came after used their parameters. We instead used a more recent adjustment of the parameters that was done using an Ab initio MD by Billeter et al. [24] for our system. The parameters are almost identical between two works with some slight changes made by Billeter and coworkers.

Molecular Dynamics Simulations

We were urged to use the Tersoff potential so that we would be able to compare our results with past works on a-Si. As mentioned before, many researchers have used Tersoff to simulate the a-Si [11][15][16][12] and a-SiH [19] and calculate their properties. We will be able to easily redo the simulations with a more accurate and costly potentials like REBO, COMB, or Reaxff once we are satisfied with the results.

Fig. 4 shows the binding (cohesive) energy of Si-H bonds from the potential that we used.

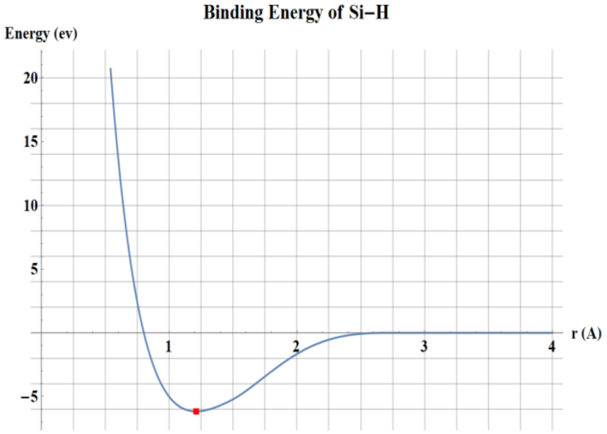

Fig. 4 Binding energy of Si-H with the Tersoff potential and parameters from [24]. $R_{eq} = 1.21\ A$

Amorphization process was done for 10 ensembles with different initial conditions (initial velocities). Thus, for each structure (ex. a-$Si_{0.9}H_{0.1}$) we generated 10 different amorphous ensembles. The most stable structure (lowest energy) was selected for further calculation of different properties including thermal conductivity, radial distribution function, the density of states (DOS) and etc. The structures were confirmed by comparing the radial distribution function (RDF) with the previous works. Fig. 5 shows the structures of a-$Si_{0.8}H_{0.2}$ with 8000 silicon atoms and 2000 hydrogen atoms.

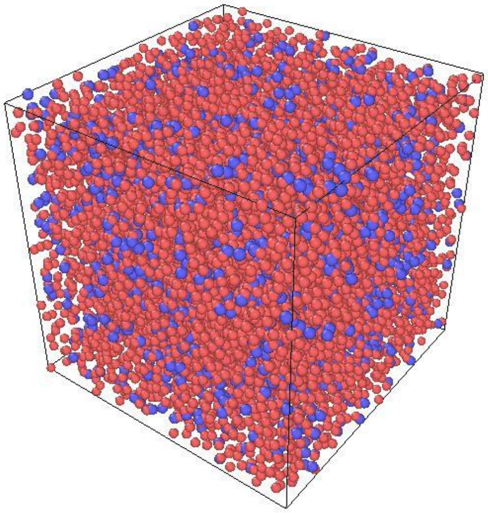

Fig. 5 The final structure of a-SiH (20% H) containing 8000 atoms.

Red spheres are silicons and blue spheres are hydrogens.

In Fig. 6 the temperature and pressure plot of a-$Si_{0.9}H_{0.1}$ during the amorphization process is shown. Since all the samples went through the same process only one sample is shown. As we can see the temperature dropped in three stages and the amplitude of the fluctuations of the pressure went down with the reduction in temperature.

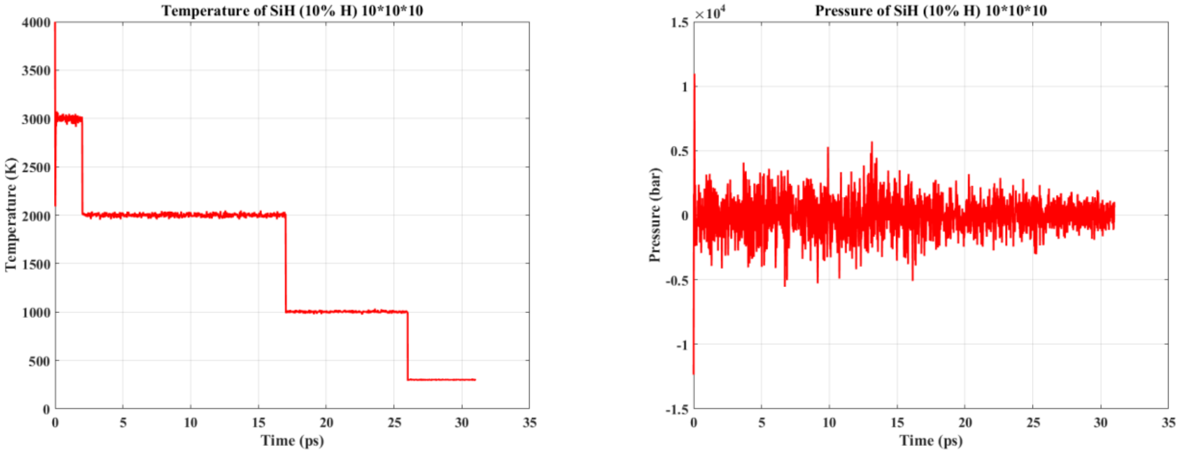

Fig. 6 Temperature and Pressure of one of the a-$Si_{0.9}H_{0.1}$ samples

One of the challenges is that hydrogen is extremely light (~28 times lighter than silicon) and that poses some problems in the simulations. Because of their small mass, hydrogens have considerably larger velocities. It means that if the timestep of the simulations is not carefully selected the assumption of the small displacements around the equilibrium position will be invalid. Therefore, the conservation of energy (in the micro-canonical ensemble) would be violated and the system keeps increasing in its total energy. It may even lead to the explosion of the system. One factor to consider is the composition of the hydrogens. As the hydrogen content increases one may require to lower the timestep to avoid the breakdown of the conservation of energy.

In Fig. 7 we drew the mean square displacement for all samples at a fixed timestep. As one can witness increasing the hydrogen in the system can result in instability of the structure. Here for the sample with 30%, the structure is moving away from the stability. The reference with regard to which the displacements are calculated is the final positions of the structures after amorphization and minimization of the energy of the structures. The jump at time 0 is due to the small displacements of atoms after putting energy into the frozen system (rising the temperature from 0 to 300 K) and the onset of the NVE simulations.

The slope of the MSD as a function of time is the diffusion coefficient. Knowing that we can say that in Fig. 7 the timestep for the 30% hydrogen structure is too large and leads to the diffusion of hydrogen atoms throughout the system.

For pure silicon structures, a timestep of around 1ft is sufficiently small; so we chose 0.5ft for our simulations. For the hydrogenated systems, we tested different timesteps and found that 0.02ft is sufficiently small for our structures.

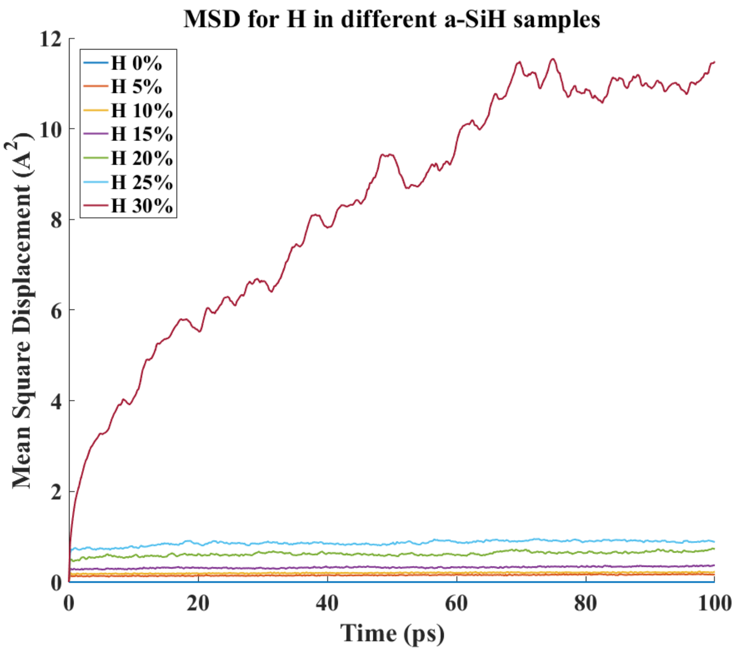

Fig. 7 Mean square displacement for a-SiH samples with different hydrogen content. The timestep is 0.05 fs for all

III. Results and discussion

Thermal conductivity and Green-Kubo formula

Now that the structures are ready, we want to calculate the thermal conductivity in our structures and observe the effect of the hydrogen in the thermal conductivity of a-SiH. In general, there are two ways to calculate thermal conductivity from MD. The first method is called non-equilibrium molecular dynamics (NEMD) which is based on the Fourier law. In NEMD we impose a temperature gradient at two ends of our system and by having the amount of the energy that is transferred, we can calculate the thermal conductivity from Fourier law.

The second method is called equilibrium molecular dynamics (EMD) and is based on the fluctuation-dissipation theorem. It uses the detailed-balance principle and is a very powerful tool in deriving some of the important properties of the system at equilibrium. Green-Kubo formala allows us to calculate thermal conductivity from atomic trajectories. It states that the thermal conductivity is the autocorrelation function of the heat currents, multiplied by some constants. The heat flux is defined as:

$$J(t) = \frac{d}{dt}\sum_i E_i r_i = \sum_i e_i v_i + \frac{1}{2}\sum_{i<j} f_{ij}.\left(v_i + v_j\right)x_{ij} = \sum_i e_i v_i + \frac{1}{2}\sum_i S_i v_i \quad (3\text{-}1)$$

Where S is the stress tensor. e_i is the sum of the kinetic and potential energy for the ith particle (local energy). The first term, $e_i v_i$ is the convective term and $S_i v_i$ is the virial term and i runs over all atoms in the supercell. Having the heat fluxes, we now can calculate thermal conductivity using Green-Kubo formula:

$$\kappa_\alpha = \frac{1}{V k_b T^2}\int_0^\infty \langle J_\alpha(0)\, J_\alpha(t)\rangle dt \quad (3\text{-}2)$$

Here α is one of the components of the thermal conductivity. In a disordered material which is supposedly isotropic one can simply average the kappa along the x, y, and z axes to find the total thermal conductivity.

Our hypothesis was that thermal conductivity of a-Si should further decrease with hydrogen doping because of their role in breaking Si-Si bonds and creating dangling bonds. Our simulations showed the opposite though. To validate our hypothesis, we calculated the thermal conductivity of our samples using the Green-Kubo formula. We ran a micro-canonical ensemble (NVE) simulation for 20 ps to find the thermal conductivities. The thermal conductivity found to plateau within the first few picoseconds (some samples took up to 5 ps for thermal conductivity to saturate). Thus, 20 ps is long enough time but not too long to bring uncertainty to our calculations.

We also ran 20 ensembles for each sample and took the average values of the thermal conductivity to reduce the variability and error. The error on the thermal conductivity calculation ranges from 1% to 1.5% for different samples (error bars are also shown in Fig. 9). Also, thermal conductivity for all the ensembles with their average is plotted in Fig. 8.

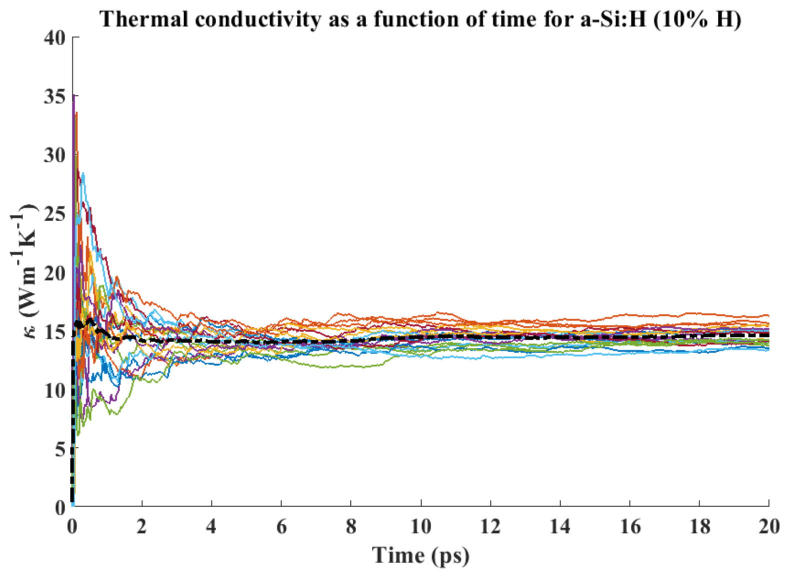

Fig. 8 Thermal conductivity vs correlation time for all the ensembles of a-Si:H (10% H). The dashed line is the average of the 20

It is important to note that thermal conductivity gradually saturates over time so we need to run for a sufficiently large correlation time to obtain the correct values for the thermal conductivity. Amorphous structures usually saturate within the first few picoseconds. Therefore, 20ps was a sufficient time for our structures (Fig. 10). Fig. 9 shows that the thermal conductivity increases with hydrogen content. Hydrogen can have competing effects on the thermal properties of the structure. On one side, it breaks some of the Si-Si bonds and creates dangling bonds. This would block some of the channels for heat flow. In other words, by breaking the network of the Si-Si, hydrogens can impede the propagation of the vibrations. Thus, the hypothesis is that the reduction in the coordination number of Si atoms can diminish the thermal conductivity [7]. On the other side, hydrogens are very lightweights and have a very high velocity compared to silicon atoms. One assumption is that their high velocity can, in fact, contribute significantly to thermal conductivity. Another possible assumption would be that hydrogenated a-Si is more crystalline and less amorphous compared to pure a-Si. This, however, strongly depends on how the sample is fabricated. We saw that in Sriraman's experiment [19] introducing hydrogen led to the crystallization of the a-Si. Now we are going to examine the validity of these assumptions. The thermal conductivity of a-Si:H samples that we prepared is shown in Fig. 9. As one can investigate thermal conductivity increases with hydrogen content.

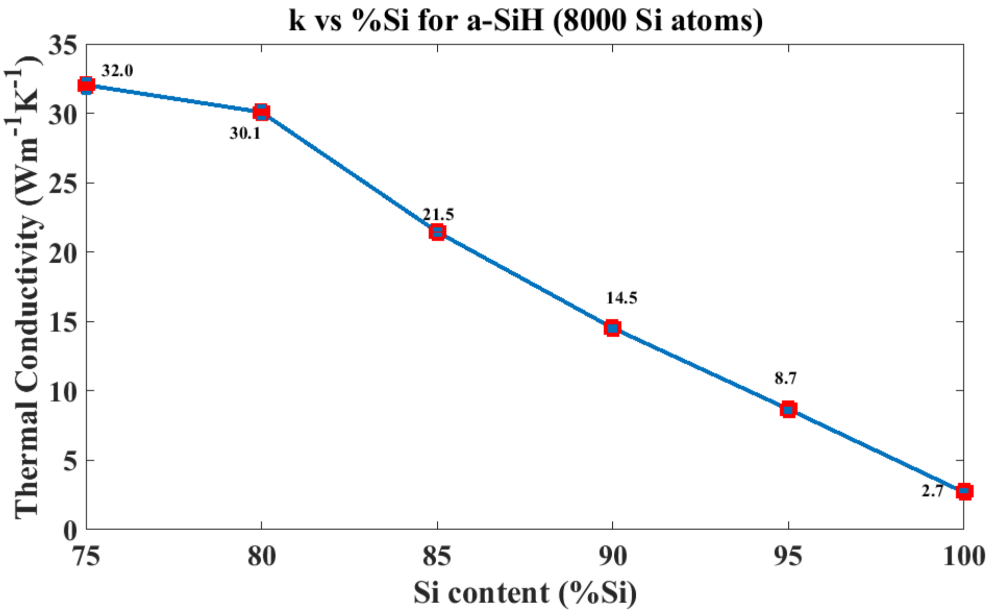

Fig. 9 Thermal conductivity calculated using G-K for different hydrogen contents. Error bars are also shown with blue bars and range from 1% to 1.5% across the samples

Now to get more insight into the effect of hydrogen doping we modified the Green-Kubo formula to separate the contributions to thermal conductivity coming from the interaction of the Si-Si, H-H, and Si-H in the system. We evaluated the heat flux for silicon atoms and hydrogen atoms separately and then rewrote the Green-Kubo formula as:

$$J(t) = J_{Si}(t) + J_H(t) \tag{3-3}$$

$$\kappa = \frac{1}{Vk_bT^2}\int_0^\infty \langle J_0\, J_t\rangle dt = \frac{1}{Vk_bT^2}\int_0^\infty \langle J_{Si_0}J_{Si_t} + J_{H_0}J_{H_t} + J_{Si_0}J_{H_t} + J_{H_0}J_{Si_t}\rangle\, dt \tag{3-4}$$

We can then write:

$$\begin{aligned}\kappa = \frac{1}{Vk_bT^2}\int_0^\infty \langle J_{Si_0}J_{Si_t}\rangle dt + \frac{1}{Vk_bT^2}\int_0^\infty \langle J_{H_0}J_{H_t}\rangle dt \\ + \frac{1}{Vk_bT^2}\int_0^\infty \langle J_{Si_0}J_{H_t} + J_{H_0}J_{Si_t}\rangle dt = \kappa_{Si} + \kappa_H + \kappa_{Si-H}\end{aligned} \tag{3-5}$$

Results and Discussion

The κ_{Si} is the part of the thermal conductivity coming from the interactions of silicon atoms with each other. Likewise, κ_H is coming from the interaction of hydrogen atoms with each other and κ_{Si-H} can be thought of as the contribution to thermal conductivity from interactions of silicon and hydrogen atoms. Fig. 10 shows our results for samples with different hydrogen contents. It is the thermal conductivity as a function of correlation time. It is evident that the κ_{Si} does not change much with increasing the hydrogen content whereas the κ_H increases considerably and is the major contributor to thermal conductivity.

It is important to mention that one cannot isolate the virial part of the heat flux for H and Si; meaning that in J_H we have the effect of silicon atoms and in J_{Si} we have the effect of hydrogen atoms. The convective term in equilibrium contributes negligibly to thermal conductivity. In the virial term the f_{ij} is the force between atom i and j. This force is effectively zero for atoms with large distances apart from each other. Thus, the greater part of the thermal conductivity comes from the atoms bonded together. In other words, it is reasonable to interpret the κ_H as the amount of the thermal conductivity coming from the H-H interactions. Likewise, κ_{Si} is coming from the Si-Si interactions and κ_{Si-H} is coming from the Si-H interactions. This method can give some insight to the role of hydrogen.

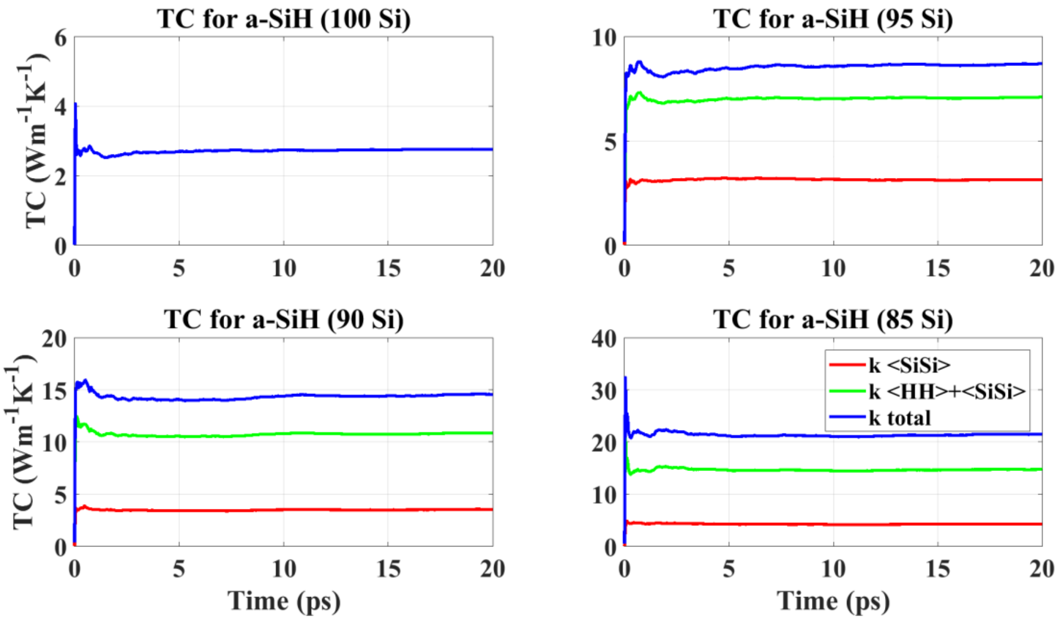

Fig. 10 Thermal conductivity contributions from different elements interactions. Blue line is the total thermal conductivity vs correlation time. Red line is the thermal conductivity from Si-Si interactions and green line is the thermal conductivity from the H-H interactions.

Results and Discussion

In Fig. 11 we plotted the thermal conductivity values obtained as a function of hydrogen atoms. Again we can investigate that the slope of κ_{Si} is very small which suggests that the majority of the thermal conductivity is coming from hydrogen atoms and their structural complexity that they bring into the structures.

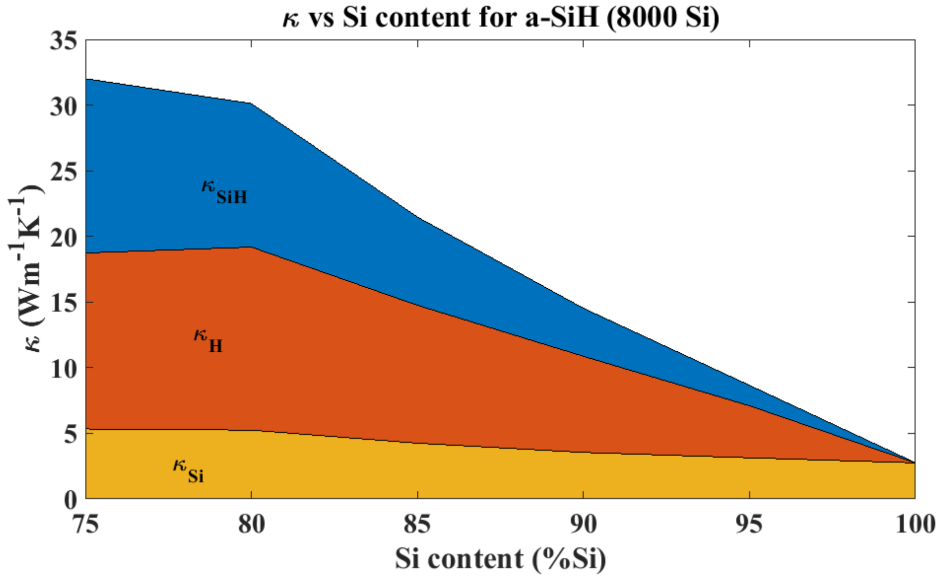

Fig. 11 Thermal conductivity separation of the contributions from pairwise interactions

It is important to mention that thermal conductivity of a-Si with Tersoff potential here is found to be 2.7 W/mK which is very close to the values in the literature. For example, He et al. [25] investigated the size effect in thermal conductivity of a-Si and found that a system with 5000 atoms is large enough to avoid any size effect. Here we have 8000 atoms which grantees that the size effect is not an issue. The value that He et al. suggest for thermal conductivity of a-Si at around 8000 atoms is ~2.6 W/mK which is reasonably in agreement with the value we found for thermal conductivity of a-Si.

Radial distribution function (RDF) and coordination number

Now to obtain a more in-depth insight into the amorphous structures we look at the radial distribution function (RDF) and coordination number. Radial distribution function (also in some references pair distribution function (PDF)) is a measure of the density, compactness, and order in a structure. It simply counts the number of pair of atoms that are placed within r, r+dr distance from each other (Fig. 12).

Results and Discussion

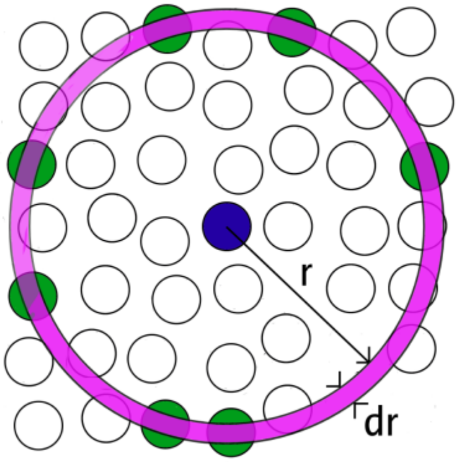

Fig. 12 Schematic of how radial distribution function is computed. Reprinted from [26]

RDF is usually plotted as a function of the distance, r. For a crystalline material, the radial distribution function has discrete peaks. Each peak indicates one set of neighboring atoms (e.x. the first peak shows the first nearest neighbor and …). But, for an amorphous solid only first few peaks are noticeable and the RDF plateaus very soon due to the lack of order in the material. In Fig. 13 we can see the RDF plot of different samples with different hydrogen content. Also, a comparison has been mad to Lakin and McGaughey's work [10] in Fig. 14. It should be noted that Larkin and McGaughey used the SW potential for their a-Si samples. There is a difference in the RDF plots that could be attributed to the potential.

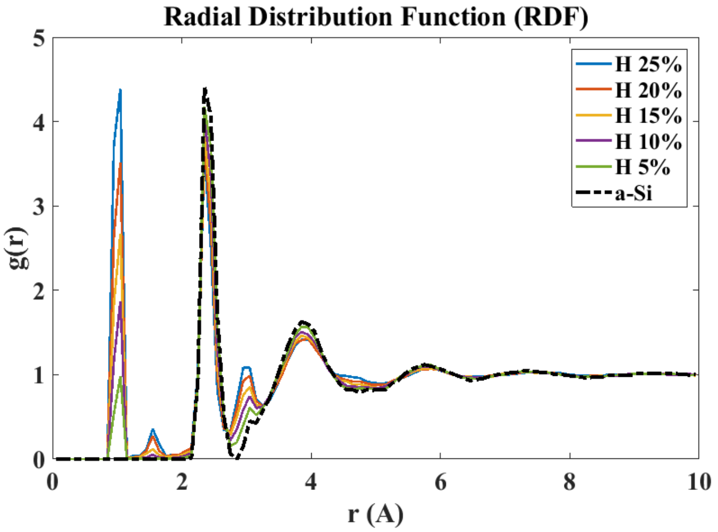

Fig. 13 RDF for samples with different hydrogen contents

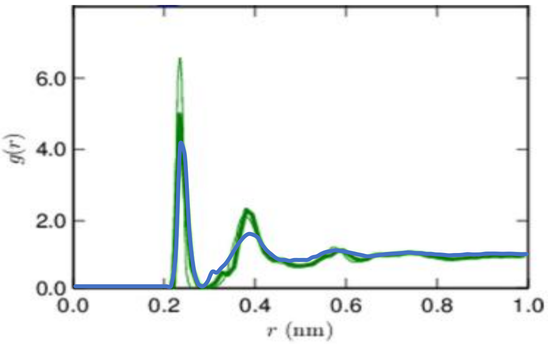

Fig. 14 Comparison of RDF of a-Si to [10]*. The blue line is our work.*

The RDF plot suggests no significant structural differences across all samples meaning that all the samples are amorphous to a good extent. The RDF of a-Si is also matching up well with the literature. To find out what each peak corresponds to we can also plot the RDF for specific atom types. We are most curious about the first few peaks so we zoom in the [0, 2.7 A] window. Fig. 15 shows the total RDF and RDF for only silicon atoms. By comparing the two diagrams we can ascertain that the second peak corresponds to the H-H bonds since it does not appear in Fig. 15-b. Similarly, we can conclude that the first peak at ~0.95 A and the third peak at ~2.35 A correspond to the Si-H and Si-Si bonds respectively.

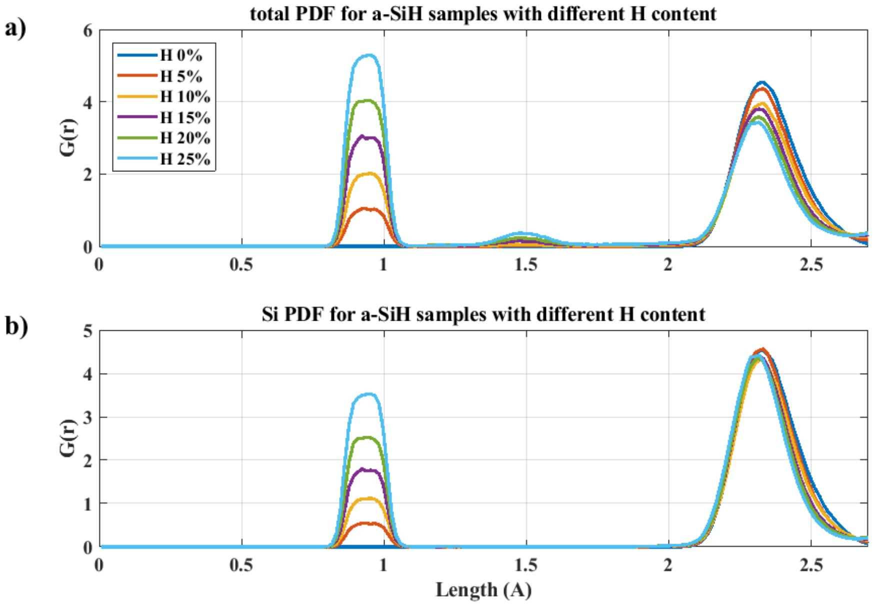

Fig. 15 RDF vs distance (r) a) total RDF averaged over all atoms b) Si RDF averaged over Si atoms. Peaks in this plot show the nearest neighbors of the Si atoms

Results and Discussion

To further corroborate our statements about the RDF plots we can take a close look at our structures. Fig. 16 shows one snapshot of a-$Si_{0.8}$:$H_{0.2}$ and we have shown some of the bond lengths on the picture. It can be seen that Si-H, Si-Si and H-H bond lengths are close to the values we drew from RDF plots.

It is important to note that the Tersoff potential that we chose led to the formation of the clusters of hydrogens in the materials which is an unreal artifact of the interatomic potential. To fix this issue and to avoid the formation of H_2 we turned off the attraction of H-H by setting the attractive force parameter to 0. This ensures that no hydrogen clustering would happen in the system. This also means that the use of "bond" for H-H interactions is not precise and hydrogens do not form covalent bonds together. Nonetheless, for the sake of the discussion, to describe the H-H interactions we used the same terminology as we used for the Si-H and Si-Si.

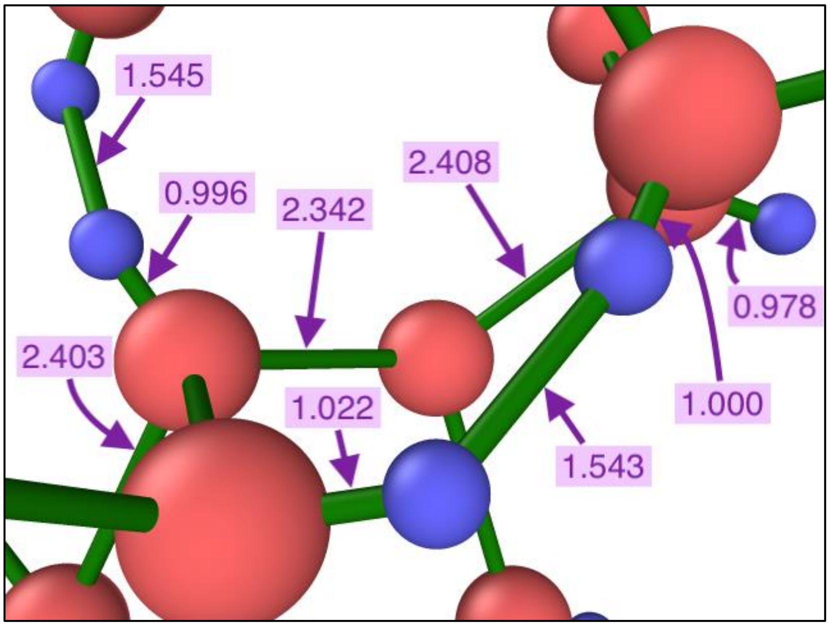

Fig. 16 bond length for one snapshot of a-Si:H (20% H). Red spheres are silicons and blue spheres are hydrogens. Bonds between hydrogens are only schematic and do not correspond to covalent bonds

We also drew the binding energy of the H-H interactions in Fig. 17. This can justify the bond length of the H-H bond which found to be ~1.5 A. The repulsion of the H-H bonds is effectively zero after 1.5 A.

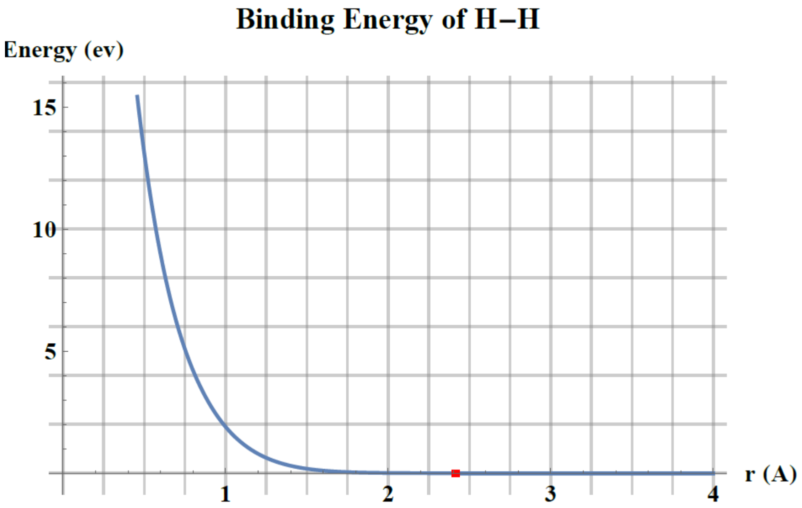

Fig. 17 binding energy of the H-H after turning off the attraction part of the potential to avoid clustering of the hydrogen atoms

We can also plot the coordination number for our samples. The coordination number is the integral of the RDF and represents the average number of the atoms that each atom in the system is bonded with as a function of distance. This is the first peak in the coordination number and normally this value is reported as the coordination number. The coordination number of silicon atoms in a perfect diamond Si is 4. For the pure a-Si also the coordination number on average is 4. In Fig. 18 the coordination number as a function of distance is drawn. The top left diagram is the average coordination number for the entire system. The top right diagram is the coordination number for Si atoms. The first peak is showing Si-H bonds and the second peak is the Si-Si bonds. The bottom left is the coordination number plot for only H atoms and the bottom right is the coordination number for Si-H bonds.

In the top right diagram one can witness that the change in the coordination number of Si atoms across different samples is very small (below 5%) which makes it hard to attribute any difference in thermal properties of the samples to the coordination number. But, we have to mention that this is the total Si coordination number including the Si-Si and Si-H bonds. In fact, the Si-Si bonds reduce linearly with increasing the hydrogen content.

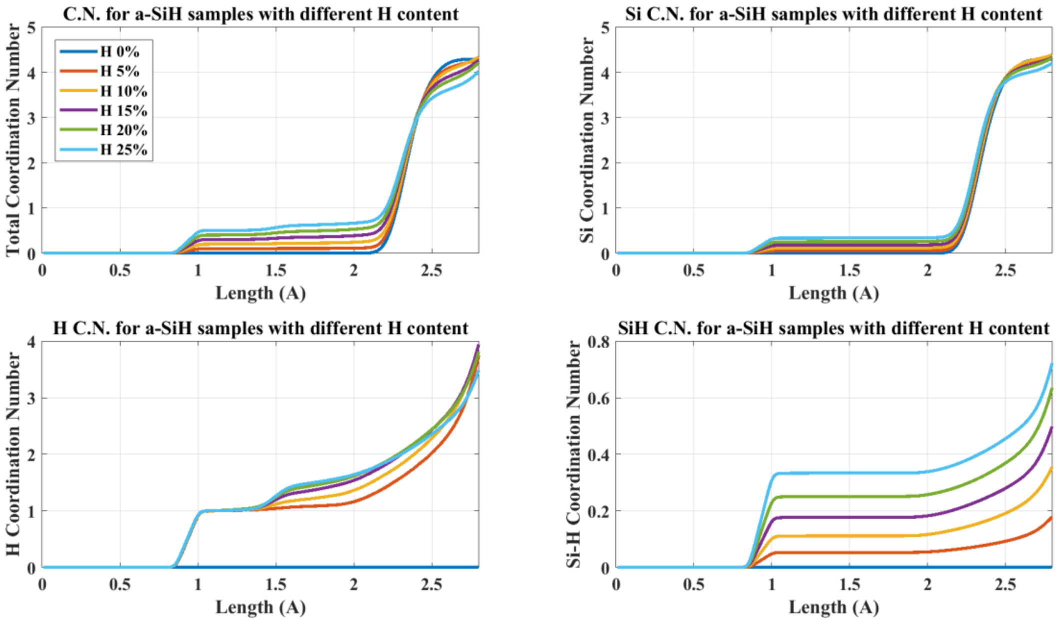

Fig. 18 The coordination number for the samples as a function of distance

Density of States

The density of states (DOS) is the number of states that exists at a certain frequency. This can apply to phonons, electrons or any vibrational modes. The vibrational density of states of a solid shows the distribution of the vibrational modes in the solid and can be derived from the autocorrelation of the atomic velocities. There are two methods to calculate the density of states from the MD simulations trajectories. The first method is to calculate the velocity autocorrelation function as:

$$V(t) = \frac{1}{N}\sum_{i=1}^{N}\frac{\langle v_i(t).v_i(0)\rangle}{\langle v_i(0).v_i(0)\rangle} \tag{3-6}$$

Now by taking the Fourier transform from VACF, we can obtain the VDOS. But there is an easier way. We can directly calculate the DOS from the Fourier transform of the velocities:

$$VDOS(\omega) = \frac{\sum_{i=1}^{N} m_i |v_i(\omega)|^2}{3Nk_B T} \tag{3-7}$$

Where, $v_i(\omega)$ is the fast Fourier transform (FFT) of the velocities. Here we used the latter approach to calculate the vibrational density of states (VDOS) for all the samples. The results are shown in Fig. 19.

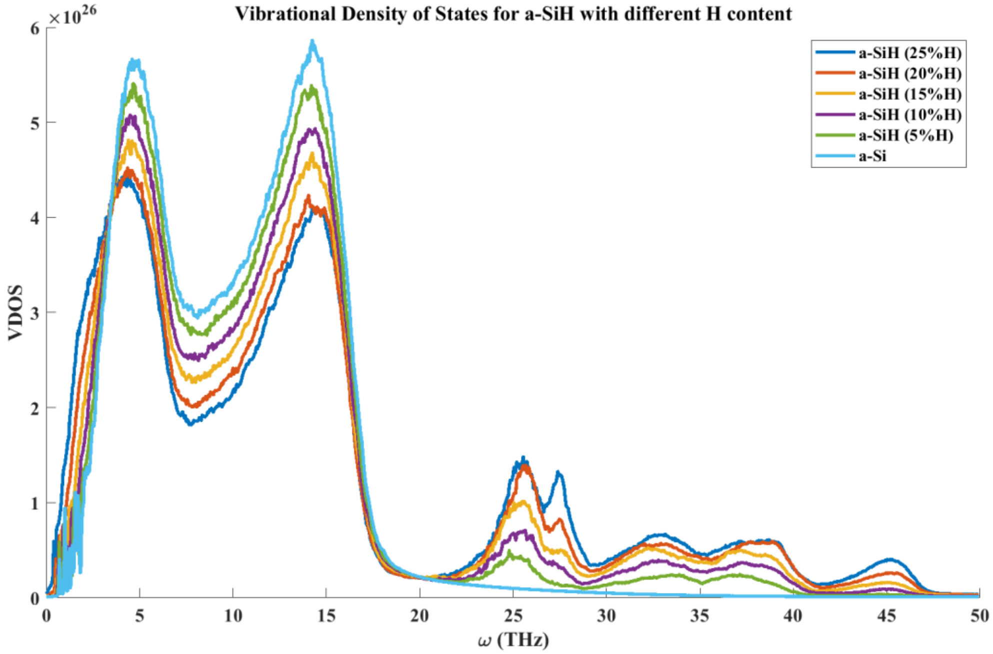

Fig. 19 DOS for a-SiH samples. We can note that as the H concentration increases, we have a shift from mid-range frequency modes to low and high-frequency modes. It qualitatively suggests a decrease in diffusons and an increase in propagons and locons with hydrogen content

The most important takeaway from the VDOS plot is that hydrogen doping does not change the distribution of vibrational modes of a-Si, rather it only adds high-frequency modes to the system which are localized modes. Therefore we can expect that these modes have a significant contribution to thermal conductivity. Also, some of the mid-range frequency modes are shifted to the high-frequency and low-frequency region. This can be interpreted as more hydrogens in the system results in more Si-H bonds whose vibrations inherently tend to be localized. Based on the results of A-F [9] of calculation of participation ratio, the cutoff frequency for locons is 70 mev (~17THz). Now we define a variable to measure the proportion of the total number of the diffusons in every sample of a-SiH to pure a-Si:

$$T_i = \frac{\left[\int_{\omega_1}^{\omega_2} DOS(\omega)d\omega\right]_{a-SiH_i}}{\left[\int_{\omega_1}^{\omega_2} DOS(\omega)d\omega\right]_{a-Si}} \tag{3-8}$$

Where the ω_2 is the cutoff frequency of the locons and diffusons and ω_1 is the cutoff frequency of the diffusons and propagons. Here we assumes ω_2 to be 17 THz and ω_1 to be 3.5 THz (we arbitrarily chose them based on previous works on a-Si, but they have to be calculated). I is the index of the sample. Fig. 20 shows that additional hydrogen in the system leads to a decrease in the propagons and diffusons.

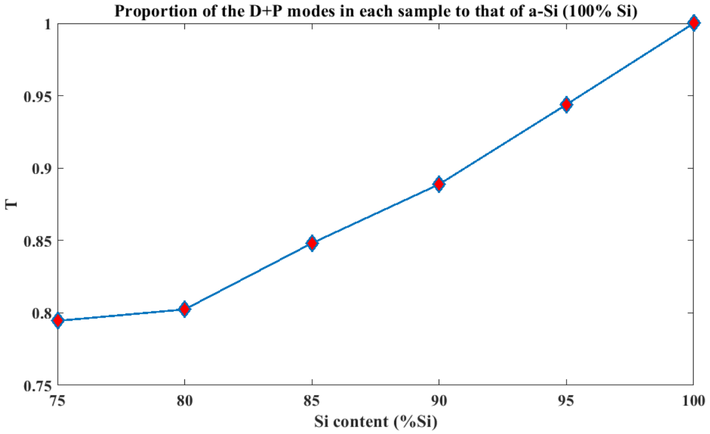

Fig. 20 Proportion of the mid-range frequency modes in each sample to that of a-Si (100% Si)

IV. Conclusion

In this study, we used molecular dynamics simulations approach to obtain a better insight into the role of hydrogen doping in the thermal conductivity of the amorphous silicon. We found that thermal conductivity increases with the hydrogen content of the samples. Although, to our knowledge, there is no experimental study on the effect of hydrogen on the thermal conductivity of a-Si by systematically varying the hydrogen concentration and measuring the thermal conductivity of the sample, there are studies that suggest high thermal conductivity for hydrogenated amorphous silicon [18]. However, a comparison should be made with utmost caution between the experimental and computational studies, especially for amorphous materials. There are so many structural complexities that come into play when working with amorphous materials. This makes it hard to confirm the similarity of the experimental samples and simulation samples. The comparison for pure silicon is easier since we have only one type of atom in the system. Experimental values reported for thermal conductivity of a-Si is ranging from below 1 to above 4

W/mK depending on how the structures were prepared and how thin the film is [27]. Our value of 2.7 W/mK for a-Si is very well in agreement with that of He et al. [11] where they found ~2.8±0.6 W/mK for a-Si for a sufficiently large system. They also used Tersoff potential and computed the thermal conductivity with G-K formula.

RDF showed that there is not much structural difference across the samples. The coordination number for Si atoms are relatively the same across all samples. Although, some of the Si-Si bonds breaks and hydrogen replace the silicon and creates dangling bonds. Seemingly, these dangling bonds alter the nature of the vibrations leading to a different distribution of modes between propagons, diffusons and locons.

We also tried to isolate the effect of hydrogens on thermal conductivity and found that hydrogens play an important role in the thermal properties of the a-Si. We concluded that Si-H bonds and H-H bonds contribute greatly to the thermal conductivity calculated using Green-Kubo formula. We argued that the high velocity of the hydrogens increases their contributions to thermal conductivity.

The results of VDOS suggests that hydrogen doping not only adds some high-frequency modes (localized modes) but slightly reduces the mid-frequency modes (Diffusons). It also slightly increases the low-frequency modes (supposedly propagons). This eventually leads to an increase in thermal conductivity. It suggests that in a-SiH the contribution of locons is considerable to thermal conductivity. However, to quantitatively corroborate this conclusion, a more systematic approach like A-F analysis or the GKMA is required.

Limitations

Here we want to point out some of the limitations to our study. The interatomic potential in any MD simulation is a major restriction to the study. Our potential does not correctly reproduce the bond lengths that was anticipated. For example, Si-H bonds in our systems are less than 1 A whereas the experimental value is reported to be 1.46 A. Sriraman et al. [19] also found a value of [1.51A, 1.65A] with Tersoff potential. Although, they used the parameters offered by Ohira et al. [28] which is an older version compared to parameters by Billeter et al. [24].

Another limitation is that by performing MD simulations we implicitly admit that we neglect the quantum effects of the atoms. It is known that the quantum-like behavior becomes important either in very low temperatures or for the lightweight elements. Hydrogen is the lightest element and exhibits quantum behavior even at room temperature. One of the problems that arises when we apply a classical point-like picture of atoms to hydrogen is that we overestimate the heat capacity. Since the heat capacity and the thermal conductivity are directly correlated, it leads to an overestimation of the thermal conductivity. Therefore, the high thermal conductivities obtained from our simulations can be partially explained by treating hydrogen classically.

Molecular dynamics simulations can be a powerful tool when applied correctly. For many materials including materials with large molecules or so many atoms in the supercell or disordered materials with no translational symmetry, it is extremely laborious to apply very accurate computational methods like DFT. Here, MD can generate good results and it is indeed used by many researchers to model this class of materials. It should be noted that sometimes results obtained by MD are not matching up excellently with the experiment in terms of the absolute values, even though they can capture the trends and reveal some important information about the material.

Future works

This work can be continued by performing a normal mode analysis. From that, we can compute the diffusivity of each mode and plot the cumulative κ of the A-F thermal conductivity and compare the κ obtained in two ways. Also, with the resort to inverse participation ratio and eigenvector periodicity we can accurately find the transition of the modal regimes. We can also compute the modal contribution to thermal conductivity which give immense insight not only into the mechanisms of heat transfer in a-Si:H but perhaps into the nature of the heat transfer in amorphous materials.

References

[1] J. Hajto and A. E. Owen, “Applications of amorphous semiconductor materials in electronics,” *Mater. Des.*, 1984.

[2] S. Reynolds and R. E. Belford, “Physics in Technology To cite this article: J. Mort,” 1980.

[3] D. G. Cahill, S. K. Watson, and R. O. Pohl, “Lower limit to the thermal conductivity of disordered crystals,” 1992.

[4] H. Ehrenreich, F. Seitz, and D. Turnbull, *Solid state physics : advances in research and applications. Volume 34*. Academic Press, 1979.

[5] D. G. Cahill, M. Katiyar, and J. R. Abelson, “Thermal conductivity of *a* -Si:H thin films,” *Phys. Rev. B*, vol. 50, no. 9, pp. 6077–6081, Sep. 1994.

[6] H.-S. Yang *et al.*, “Anomalously high thermal conductivity of amorphous Si deposited by hot-wire chemical vapor deposition.”

[7] J. L. Braun *et al.*, “Breaking network connectivity leads to ultralow thermal conductivities in fully dense amorphous solids,” *Appl. Phys. Lett.*, vol. 109, no. 19, pp. 0–5, 2016.

[8] P. B. Allen and J. L. Feldman, “Thermal conductivity of disordered harmonic solids,” 1993.

[9] P. B. Allen, J. L. Feldman, J. Fabian, and F. Wooten, “Diffusons, Locons, Propagons: Character of Atomic Vibrations in Amorphous Si,” 1999.

[10] J. M. Larkin and A. J. H. Mcgaughey, “Thermal conductivity accumulation in amorphous silica and amorphous silicon,” *Phys. Rev. B*, vol. 89, no. 73, 2014.

[11] Y. He, D. Donadio, and G. Galli, “Heat transport in amorphous silicon: Interplay between morphology and disorder,” *Appl. Phys. Lett*, vol. 98, p. 144101, 2011.

[12] J. Moon, B. Latour, and A. J. Minnich, “Propagating elastic vibrations dominate thermal conduction in amorphous silicon,” *Phys. Rev. B*, vol. 97, p. 24201, 2018.

[13] W. Lv, A. Henry, and G. W. Woodruff, “Non-negligible Contributions to Thermal Conductivity From Localized Modes in Amorphous Silicon Dioxide,” *Nat. Publ. Gr.*, 2016.

[14] R. Biswas, A. M. Bouchard, W. A. Kamitakahara, G. S. Grest, and C. M. Soukoulis ', "NUMBER 22 PHYSICAL REVIEW LETTERS," 1988.

[15] H. R. Seyf, A. Henry, and G. W. Woodruff, "A method for distinguishing between propagons, diffusions, and locons," *Nanoscale Therm. Transp. J. Appl. Phys.*, vol. 120, p. 121904, 2016.

[16] W. Lv and A. Henry, "Direct calculation of modal contributions to thermal conductivity via Green–Kubo modal analysis," *New J. Phys.*, vol. 18, no. 1, p. 013028, Jan. 2016.

[17] L. Isaeva, G. Barbalinardo, D. Donadio, and S. Baroni, "Modeling heat transport in crystals and glasses from a unified lattice-dynamical approach," 2019.

[18] X. Liu *et al.*, "High Thermal Conductivity of a Hydrogenated Amorphous Silicon Film," vol. 70, 2009.

[19] E. S. A. Saravanapriyan Sriraman, Sumit Agarwal and & D. Maroudas, "Mechanism of hydrogen-induced crystallization of amorphous silicon," *Nature*, vol. 418, no. 62, pp. 62–65, 2002.

[20] J. D. Gale and A. L. Rohl, "The General Utility Lattice Program (GULP)," *Mol. Simul.*, vol. 29, no. 5, pp. 291–341, May 2003.

[21] A. Stukowski, "Visualization and analysis of atomistic simulation data with OVITO–the Open Visualization Tool," *Model. Simul. Mater. Sci. Eng.*, vol. 18, no. 1, p. 015012, Jan. 2010.

[22] J. Tersoff, "Modeling solid-state chemistry: Interatomic potentials for mnlticomponent systems," *Phys. Rev. B*, vol. 39, no. 8, 1989.

[23] T. I. and T. A. Tatsuya Ohira, "Molecular Dynamics Simulation of Hydrogenated Amorphous Silicon with Tersoff Potential," *Amorph. silicon Technol.*, vol. 336, 1994.

[24] S. R. Billeter, A. Curioni, D. Fischer, and W. Andreoni, "Ab initio derived augmented Tersoff potential for silicon oxynitride compounds and their interfaces with silicon," *Phys. Rev. B*, vol. 73, 2006.

[25] Y. He, D. Donadio, and G. Galli, "Heat transport in amorphous silicon: Interplay between

morphology and disorder," *Appl. Phys. Lett.*, vol. 98, no. 14, p. 144101, Apr. 2011.

[26] "Radial distribution functions." [Online]. Available: http://isaacs.sourceforge.net/phys/rdfs.html. [Accessed: 08-Jul-2019].

[27] J. L. Braun *et al.*, "Size effects on the thermal conductivity of amorphous silicon thin films," *Phys. Rev. B*, vol. 93, 2016.

[28] T. Ohira, O. Ukai, T. Adachi, Y. Takeuchi, and M. Murata, "Molecular-dynamics simulations of SiH3 radical deposition on hydrogen-terminated silicon (100) surfaces," *Phys. Rev. B*, vol. 52, no. 11, pp. 15–1995.

Appendix A: Size effect on thermal conductivity *κ*

To find out the size effect on the thermal conductivity on our structures, we did all the simulations for two simulation boxes. Based on the work by He et al. [25] in which they investigated the effect of number of the atoms in the simulation box on the thermal conductivity from EMD, we expected to see no significant difference the calculated values after 5000. Therefore, we first used a c-Si of 7×7×7 with a total of 2744 Si atoms for the basis of our simulations. Then we also redid everything with 10×10×10 c-Si supercell with a total of 8000 silicon atoms. Some samples depending on the hydrogen content went passed 10000 atoms (ex. a-Si:H 20% H). We saw no difference in the calculated thermal conductivity (Fig. 21). This seems compelling enough that we had no size effect issue in our calculations.

To be more cautious one can go up to 15000-20000 atoms supercell and further validate that our samples were sufficiently large to produce reliable results.

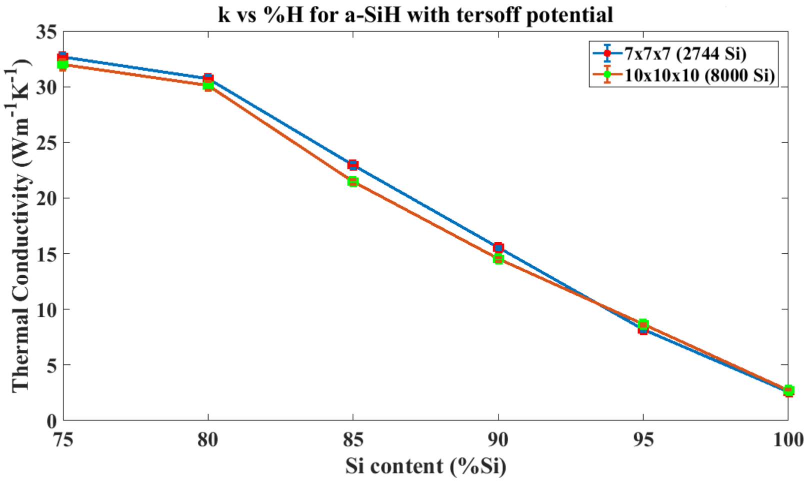

Fig. 21 Size effect investigation for two sets of samples. No considerable difference in the calculated κ

Appendix B: Volume change across the samples

The variation in volume is also investigated. It was found that the volume changes relatively exponential with hydrogen. The changes in volume with hydrogen content with respect to pure a-Si is plotted in Fig. 22. The effect of volume should be carefully considered particularly for interpreting the results from the DOS. We divided the DOS by volume to get the DOS per volume to be able to correctly compare the samples.

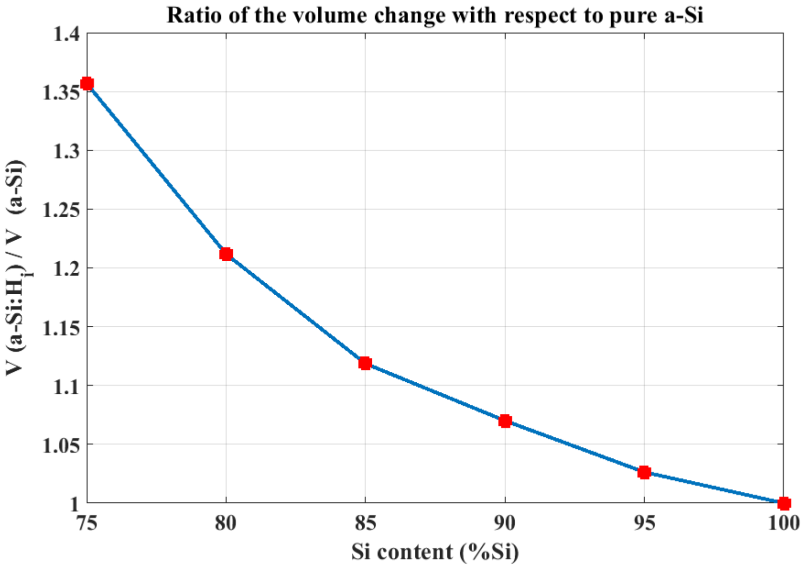

Fig. 22 change in volume with hydrogen content of the samples.